GLOBAL BIOGEOCHEMICAL CYCLES, VOL. 22, GB4004, doi:10.1029/2007GB003054, 2008

Click Here for Full Article

Glacial-interglacial variations in marine phosphorus cycling: Implications for ocean productivity

I. Tsandev,[1] C. P. Slomp,[1] and P. Van Cappellen[1]

Received 4 July 2007; revised 9 April 2008; accepted 21 May 2008; published 10 October 2008.

[1] Using a box model of organic carbon (C) and phosphorus (P) cycling in the global ocean, we assess the effects of changes in the continental supply of reactive P, oceanic mixing, and sea level on the marine P cycle on glacial-interglacial timescales. Our model results suggest that mixing is a dominant forcing during early glaciation, causing retention of P in the deep ocean, thereby lowering primary production and associated organic C and P burial. Sea level fall is the dominant forcing during late glaciation, when reduced coastal trapping of reactive P enhances its transfer to the open ocean, restoring primary production and P burial. During postglacial periods, changes in circulation and weathering dominate open ocean processes and oceanic primary production peaks. As primary production is reduced upon glaciation, changes in the marine P cycle are unlikely to drive enhanced primary production and CO_2 drawdown during glaciation.

Citation: Tsandev, I., C. P. Slomp, and P. Van Cappellen (2008), Glacial-interglacial variations in marine phosphorus cycling: Implications for ocean productivity, *Global Biogeochem. Cycles*, *22*, GB4004, doi:10.1029/2007GB003054.

1. Introduction

[2] Cyclicity of 100,000 years in atmospheric CO_2 concentration is discernable as far back as 740,000 years ago [*Petit et al.*, 1999; *Siegenthaler et al.*, 2005]. These changes in atmospheric pCO_2 are believed to be caused, to a large extent, by changes in the ocean/atmosphere exchange of CO_2, but there is not yet agreement on the underlying mechanisms. One suggested mechanism is a glacial increase in the strength of the biological pump as a result of increased nutrient availability [*Broecker*, 1982; *Sigman and Boyle* 2000; *Peacock et al.*, 2006].

[3] The debate over the role of the "nutrient-CO_2 connection" [*Broecker*, 1982] has recently been revived by the downward revision of the oceanic residence time of reactive phosphorus (P) [*Latimer et al.*, 2006], with estimates now ranging from 8.8 to 38 ka [*Wallmann*, 2003; *Ruttenberg*, 1993, 2003] instead of the previously assumed 80 to 100 ka [*Froelich et al.*, 1982; *Broecker*, 1982]. Thus, on timescales of glacial-interglacial cycles, the availability of P could exert a major control on global oceanic primary productivity [*Filippelli*, 2002; *Holland*, 1984; *Tyrrell*, 1999; *Compton et al.*, 2000]. While physical and biological mechanisms for glacial-interglacial forcings on the carbon cycle itself are widely studied [*Archer et al.* 2000a; *Heinze et al.*, 1999; *Ridgwell*, 2001; *Archer et al.*, 2000b], the effects of these cycles on growth limiting nutrients have received less attention. A handful of modeling studies have estimated the consequences for the marine cycles of nitrogen [*Christensen*, 1994; *Deutsch et al.*, 2004] and iron [*Ridgwell*, 2003; *Lefevre and Watson*, 1999].

[4] There is some debate over the key limiting nutrient exerting overall control on the organic carbon cycle. *Sigman et al.* [1999] propose nitrate utilization in the surface Antarctic was higher during the last ice age, using that to account for CO_2 drawdown. *Latimer and Filippelli* [2001] propose a micronutrient connection, suggesting that iron from hemipelagic sediments could have stimulated primary production during glacial periods. However, based on a simple theoretical study of nutrient co-limitation, *Tyrrell* [1999] concludes that while surface waters can be more depleted in nitrate than in phosphate in the steady state, it is the external input of phosphate which controls longer-term primary production in the global ocean, such as over glacial times.

[5] *Wallmann* [2003] proposes that the response of the marine P cycle to fluctuations in sea level and terrigenous inputs results in a positive feedback loop, due to the redox dependence of P regeneration. An initial increase in primary production can cause enhanced respiratory oxygen consumption in the water column; low-oxygen waters in turn lead to preferential regeneration of reactive P, culminating in a further enhancement of primary production. Below a threshold value in deep water oxygen concentration (100 μM), this feedback may allow even small increases in organic matter export to induce a rapid drop in the oxygen level. The corresponding P-driven spike in productivity could then drive the ocean to eutrophic conditions and cause it to become nitrogen (N) limited [*Wallmann*, 2003]. However, on glacial-interglacial timescales, the deep ocean never reaches the critical level of oxygen depletion and thus remains P limited. The study of *Wallmann* [2003] focuses primarily on the transition from interglacial to glacial con-

[1]Department of Earth Sciences-Geochemistry, Faculty of Geosciences, Utrecht University, Utrecht, Netherlands.

Copyright 2008 by the American Geophysical Union.
0886-6236/08/2007GB003054$12.00

ditions and it does not consider the effect of circulation during glacial times. However, ocean circulation is likely a key factor in glacial-interglacial nutrient cycling and pCO_2 trends [*Toggweiler*, 1999; *François et al.*, 1997; *Sigman and Boyle*, 2000; *Broecker et al.*, 2004; *Peacock et al.*, 2006; *Willamowski and Zahn*, 2000].

[6] Using a 1-box model of the ocean, *Van Cappellen and Ingall* [1994] showed that a reduction in oceanic circulation (mixing between deep and shallow waters) causes an initial drop in primary production, because the immediate supply of dissolved P to the surface waters is decreased. However, with time, as oxygen levels decrease, the deep water builds up phosphate and the upward transport of P is enhanced, boosting primary production. So the short-term and long-term effects of changes in circulation differ, and the effect of oceanic circulation on primary production is highly dependent on the timescale of the changes in circulation and on the oceanic residence time of the limiting nutrient. *Slomp and Van Cappellen* [2007] show that the response of the marine P cycle to oceanic circulation is further complicated when considering the continental margins separately, because of their differing biogeochemical dynamics from those of the open ocean [*Slomp and Van Cappellen*, 2007] and their high capacity for P storage [*Ruttenberg*, 1993; *Howarth et al.*, 1995].

[7] We note here that circulation is not explicitly described in the box models described above. Rather, the effect of circulation is represented by the degree of mixing between deep waters and surface waters. Increased circulation thus is associated with enhanced exchange between surface and deep waters. It is this aspect of circulation only which is represented in box models and the model used for this study.

[8] In the present study, we use a modified version of the 4-box model of *Slomp and Van Cappellen* [2007] and incorporate the changes in oceanic mixing in a generic full glacial-interglacial transition scenario. This allows us to examine the interaction effects of circulation with other forcings, in particular sea level change and variations in dust and river inputs of reactive P to the ocean. We observe changes in the speciation of sedimentary P burial and examine the role of the oceanic residence time of phosphorus. By assuming that phosphorus controls primary production, we further determine the effects on the ocean organic C cycle and the possible link to climate. In particular, we test the hypothesis of a P driven boost in primary production during times of glaciation.

2. Glacial-Interglacial Climate Change

[9] In order to simulate changes in the marine P cycle and the associated organic carbon cycle, it is necessary to first properly identify and constrain the environmental/climate forcings which likely perturb these biogeochemical cycles during glaciations.

[10] Besides the well-documented variations in temperature, four other global climate forcings could affect the global phosphorus cycle during glacial-interglacial transitions. These are sea level fluctuations, changes in riverine and eolian reactive P supply to the open ocean, and changes in oceanic mixing, particularly the intensity of deep water upwelling. Here we review the state of knowledge on the variability of these factors across glacial-interglacial transitions and outline a climate change scenario for the last glacial-interglacial cycle.

2.1. Sea Level

[11] Sea level is perhaps the best constrained variable of glacial-interglacial cycles. As such, it is used as the time benchmark, as it inversely correlates to ice sheet volume and global temperature. According to paleoproxy records [*Fairbanks*, 1989; *Lambeck and Chappell*, 2001; *Siddall et al.*, 2003], sea level dropped by up to 120 m at the Last Glacial Maximum (LGM): 20,000 years before present. As the continental shelf extends to approximately 250 m depth (average depth of 130 m), a 120 m sea level drop is equated to a recession of the shoreline equivalent to a 50% loss of continental shelf from estimates made by *Peltier* [1994] and *Wallmann* [2003]. Transient, high-frequency fluctuations in sea level are not represented here. We simply follow the effects of the net change in coastal volume during glaciation.

2.2. Riverine Supply of Reactive P

[12] *Föllmi* [1995] reports that changes in chemical weathering (as the main long-term source of dissolved bioavailable phosphorus) were driven by changes in total continental weathering. By analyzing changes in exposed areas and changes in weathering processes, *Kump and Alley* [1994] concluded that the supply of reactive material from land at the LGM was not significantly different from the present. However, ice age temperatures are thought to have reduced precipitation and evaporation to about 10–15% below modern values [*Kump and Alley*, 1994; *Ganopolski et al.*, 1998]. It is this change in the hydrological cycle, and not the weathering regime on land, which leads to a similar decrease in riverine runoff and supply of organic carbon to the oceans [*Ludwig et al.*, 1999; *Ludwig and Probst*, 1999; *Hay and Southam*, 1977]. In this study, we employ a 10% drop in the riverine supply of reactive P from the continents during glaciation. The onset of decline in chemical weathering during glaciation would have occurred after sea level and temperature had already begun to fall.

2.3. Dust

[13] The general trend of eolian input to the oceans during glaciation is a dust flux increase due to the cold, arid, windy climates of the glacial period and the increased area of exposed land [*Delmonte et al.*, 2004; *Broecker*, 1997; *An et al.*, 1991; *Rea et al.*, 1994]. Given that dust flux represents a small fraction of total P input to the coastal zone (<10% according to *Lerman* [1994] and *Graham and Duce* [1982]), the eolian input is mainly of importance for the surface waters of the open ocean [*Benitez-Nelson*, 2000; *Graham and Duce*, 1982]. The reported increase in dust supply to the ocean ranges from 1.5 to 3 times greater during the LGM than interglacial values [*Hesse*, 1994; *An et al.*, 1991; *Anderson et al.*, 2006; *Wallmann*, 2003]. Suggestions of an order of magnitude greater dust supply to the open ocean at the LGM have also been put forward [*Harrison et al.*, 2001; *LeGrand et al.*, 1988; *Kohfeld and Harrison*, 2001; *Delmonte*

Table 1. List of Studies Comparing Oceanic Circulation During the Last Glacial to Current (Interglacial) Oceanic Circulation[a]

Area/Location	Method/Proxy	Circulation State Relative to Today[b]	Reference
Cariaco Basin	^{14}C + box model	-	*Hughen et al.* [2004]
North Atlantic	Modeling	-	*Seidov et al.* [1996]
General	modeling and ^{14}C	-	*Meissner et al.* [2003]
Florida Straits	$\delta^{18}O$ in benthic foraminifera	-	*Lynch-Stieglitz et al.* [1999]
Southern Ocean	$\delta^{15}N$, ^{230}Th-normalized opal fluxes, biogenic Ba rain rate, $^{231}Pa/^{230}Th$, authigenic U	-	*François et al.* [1997]
General	various (pertains to a different period)	-	*Sigman et al.* [2004]
Subarctic North Pacific	Biogenic Ba	-	*Jaccard et al.* [2005]
General	Box models	-	*Toggweiler* [1999]
General	Box model + CO_2 record	-	*Peacock et al.* [2006]
General	LGS (general circulation model)	-	*Winguth et al.* [2000]
General	$^{231}Pa/230^{Th}$ ratios + circulation biogeochemistry model	-	*Marchal et al.* [2000]
General	Summary of various studies	−/+	*Corliss et al.* [1986]
General	$^{14}C/C$, benthic and planktonic foraminifera	≈	*Broecker* [1987]
General	Ocean general circulation model	≈	*Paul and Schäfer-Neth* [2003]
West Equatorial Pacific	$^{14}C/C$	≈	*Broecker et al.* [2004]
General	Modeling	≈	*Ganopolski et al.* [1998]
Atlantic	$^{231}Pa/^{230Th}$	≈/+	*Yu et al.* [1996]
Northwest Pacific	$\delta^{13}C$ and $\delta^{18}O$ in cibicidoides	+	*Keigwin* [1998]
Equatorial Pacific	C_{37-39} alkenones	+	*Lyle et al.* [1992]
General	18-box model	+	*Wunsch* [2003]

[a]Locations and methodology are also given.
[b]Symbols indicate: "≈" = similar, "+" = increase, "−" = decrease.

et al., 2004]. The high estimates, however, are based on paleorecords of bulk dust deposition in ice cores, which do not necessarily reflect the trends in eolian reactive P supply.

[14] The dust trend in our baseline model scenario is in line with flux estimates of *Wallmann* [2003] and *Anderson et al.* [2006], namely a doubling of the dust flux of reactive P during glacial periods. According to dust records in ice cores, the eolian flux increased primarily during the second half of the glacial period [*Petit et al.*, 1999; *Broecker and Henderson*, 1998]. *Peacock et al.* [2006] also propose that, if dust plays a role, it is only during the later phase (second half) of glaciation.

2.4. Mixing

[15] Mixing, as the term is used here, refers to the exchange between water masses on the surface ocean and the deep sea, as well as upwelling on the coast; it is a measure of the connectivity between the water masses and their ability to exchange nutrients and oxygen. Note that oceanic mixing is a complex process which is heterogeneously distributed throughout the ocean, a feature which cannot be captured with a 4-box model. There has been quite some debate concerning oceanic mixing during glacial times [*Archer et al.*, 2000a; *Peacock et al.*, 2006] as summarized in Table 1. Some of the disagreement stems from the methodologies used for estimating paleocirculation. Relying on paleoproxy tracer distributions (such as $\delta^{13}C$, $\delta^{18}O$, and CO_2 signatures) and inverse modeling, earlier reconstructions have been questioned recently by, for example, *Rutberg and Peacock* [2006], *LeGrand and Wunsch* [1995], and *Bigg et al.* [1998], who show sensitivity to boundary conditions and multistability of circulation model solutions.

[16] Glacial mixing scenarios fall into three main categories (Table 1) based largely on overturning circulation: reduced intensities by up to 30–40% [*Winguth et al.*, 2000; *Meissner et al.*, 2003], similar intensity as today, and increased mixing rates. The dominant opinion, however, is one of a less ventilated glacial ocean [*Sigman et al.*, 2004; *Rahmstorf*, 2002; *Jaccard et al.*, 2005; *François et al.* 1997; *Toggweiler*, 1999]. Recent work of *Yu et al.* [1996] and *Wunsch* [2003], corroborated by earlier propositions of *Broecker* [1987], suggest that if mixing had slowed down, it could not have been significantly slower than today. *Marchal et al.* [2000] expand on the findings of *Yu et al.* [1996] by determining a lower bound on glacial mixing; connectivity between water masses during glacial times could have been no more than 30% weaker than today's.

[17] Whatever the debate over open ocean water exchange may be, the case for increased coastal upwelling is particularly strong due to the increased geostrophic circulation (particularly Eckman flow) caused by stronger Northern Hemisphere trade winds of the glacial period [*Ganopolski et al.*, 1998; *Wunsch*, 2003; *Jewell*, 1994]. Such a scenario is supported by regional coastal studies such as those of *West et al.* [2004], *Romero et al.* [2003], and *Martinez et al.* [1999]. Therefore, the glacial ocean likely saw less water mixing between the surface and deep ocean but the coastal waters received a greater supply of upwelled deep water.

[18] The timing of mixing changes implemented in our scenario is taken after *Peacock et al.* [2006], who propose that an early decrease in circulation, during the first 10 ka of glaciation, and a return to full mixing in the last 10 ka (deglaciation) of the glacial-interglacial cycle, agree best with recorded atmospheric CO_2 trends. Reduced circulation through most of the glacial is also in accordance with results of *Hughen et al.* [2004], and a similar timing of the circulation perturbation has been employed in carbon box modeling efforts [*Köhler and Fischer*, 2006].

2.5. Sea Surface Oxygen

[19] An important effect of mixing is ventilation, the supply of oxygen to the deep ocean. As temperature

decreases, oxygen solubility in the surface waters increases, and downwelled waters are enriched in oxygen, which may offset the effect of reduced downwelling on ventilation. For the purposes of representing a realistic ventilation rate, we include the oxygen solubility dependence on temperature [*Pilson*, 1998]. We represent this effect by modulating the sea surface oxygen content using the sea surface temperature (SST) change during glaciation and deglaciation. The SST at the LGM is reported to be 1.5–7°C cooler than global average SST for preindustrial oceans [*CLIMAP Project Members*, 1981; *McManus et al.*, 1999; *Paul and Schäfer-Neth*, 2003], with most recent estimates converging on a 4°C cooling [*Kageyama et al.*, 2006].

3. Model Description

3.1. The 39 ka Model

[20] The 4-box model of *Slomp and Van Cappellen* [2007] explicitly represents the proximal and distal coastal zones, the surface open ocean, and the deep ocean. Steady state water, organic carbon (C), oxygen (O), and phosphorus (P) cycles are parameterized to interglacial conditions (preindustrial Holocene), imposing a 39,000 year (39 ka) oceanic residence time for P. The phosphorus cycle drives the organic carbon cycle, by assuming P limitation on marine primary production. This is a reasonable simplifying assumption given the spatial and temporal scales considered [*Holland*, 1984; *Tyrrell*, 1999; *Compton et al.*, 2000]. The model calculations presented also assume a constant Redfield ratio of P fixation into organic matter (OM). It is important to note, however, that non-Redfield behavior may affect nutrient inventories, and therefore nutrient limitation itself [*Sigman and Boyle*, 2000; *Falkowski*, 1997].

[21] The model accounts for the transformation of soluble reactive phosphorus (SRP) into particulate organic phosphorus (POP) and fish biomass, with separate parameterizations for the coastal zones and the open ocean. Three separate forms of buried phosphorus are considered; calcium-associated P (CaP), iron-bound P (FeP), and organic P (POP). The burial of both FeP and POP in deep-sea sediments is dependent on deep water oxygenation. This is also the case for the burial of organic C (POC) and the burial ratio POC:POP [*Slomp and Van Cappellen*, 2007].

[22] The only modification from the model of *Slomp and Van Cappellen* [2007] consists of an explicit representation of the eolian input of reactive P input to the ocean. To this end, the riverine reactive P flux is lowered slightly (11%), and the corresponding reactive phosphorus is introduced as a dust flux into the open ocean [*Graham and Duce*, 1982].

[23] Export of POP and fish biomass to the deep ocean is calculated as the fraction of the primary production rate and, for POP, the input from the adjacent landward reservoir. This description of export production does not take into account ballasting effects of settling material [e.g., *De La Rocha and Passow*, 2007; *Boyd and Trull*, 2007].

3.2. The 13 ka Model

[24] Recent studies have yielded considerably lower estimates of the residence time of reactive P in the oceans [*Benitez-Nelson*, 2000; *Ruttenberg*, 1993]. We therefore also consider a version of the phosphorus cycle with a shorter residence time of 13 ka. The water cycle and oxygen cycle are kept the same as in the 39 ka model. The 13 ka phosphorus cycle is adjusted by tripling the input of riverine reactive P from the continents (maintaining atmospheric input the same) and adjusting the burial of phosphorus and organic carbon. Total organic carbon burial increases from 7.9 Tmol/a in the 39 ka residence time model (80% on the continental margins and 20% in the deep ocean) to 13.3 Tmol/a in the 13 ka residence time model (90% on the continental margins and 10% in the deep ocean) [*Hedges and Keil*, 1995].

[25] In order to accommodate the increased burial of P within the constraints reported in the literature (particularly total C burial and C/P burial ratios in shelf and deep ocean sediments), the partitioning of buried reactive P phases is modified relative to the 39 ka residence time P cycle. In the 39 ka model, P burial is characterized by CaP:FeP:POP = 50:25:25 everywhere in the ocean. In the 13 ka model, burial in the coastal zones is characterized by CaP:FeP:POP = 58:21:21 [*Slomp et al.*, 1996] and that in the deep ocean by CaP:FeP:POP = 86:7:7 [*Anderson et al.*, 2001]. The latter ratios represent the extreme values for reported buried P speciation. This shift is accompanied by a shift in the total organic carbon to total reactive phosphorus burial ratio (C_{org}/P_{reac}) in coastal sediments from 400 (39 ka model) to 300 (13 ka model). Some internal (unconstrained) fluxes are also adjusted to maintain mass balance. All other constraints are kept identical between the two versions of the P cycle. The steady state of the reduced residence time version of the P cycle is shown in Figure 1, and the resulting modifications to the organic carbon cycle (from the 39 ka model) are listed in Table 2.

[26] Given the currently available estimates of organic matter (OM) burial rates and P partitioning in marine sediments, a 13 ka oceanic residence time is at the edge of the constraints imposed by budgets for the global oceanic P and organic C cycles. In particular, a residence time lower than 12 ka, and the corresponding higher burial of reactive P, would require a relative contribution of CaP in deep-sea sediments and a total POC burial exceeding the highest reported values so far (80–90% CaP, *Anderson et al.* [2001]; 13.3 Tmol POC/a, *Hedges and Keil* [1995]).

3.3. Model Sensitivity to Forcings

3.3.1. Response to Sea Level Fluctuations

[27] As the best constrained forcing parameter, sea level is treated separately and varied according to the prescribed scenario outlined in section 2.1. The model response to sea level fall and rise is shown in Figure 2. Results are given for the two oceanic residence times of reactive P (39 and 13 ka). For both residence times the model responds in the same qualitative way to the sea level forcing. The main difference is that the shorter residence time is more responsive to the forcing.

[28] Upon sea level fall (glacial stage), the retention capacity of the coastal ocean for reactive P through burial decreases, due to the shrinking of the shelf. The net effect is thus a transfer of reactive P to the open ocean. This stimulates open ocean primary production and export pro-

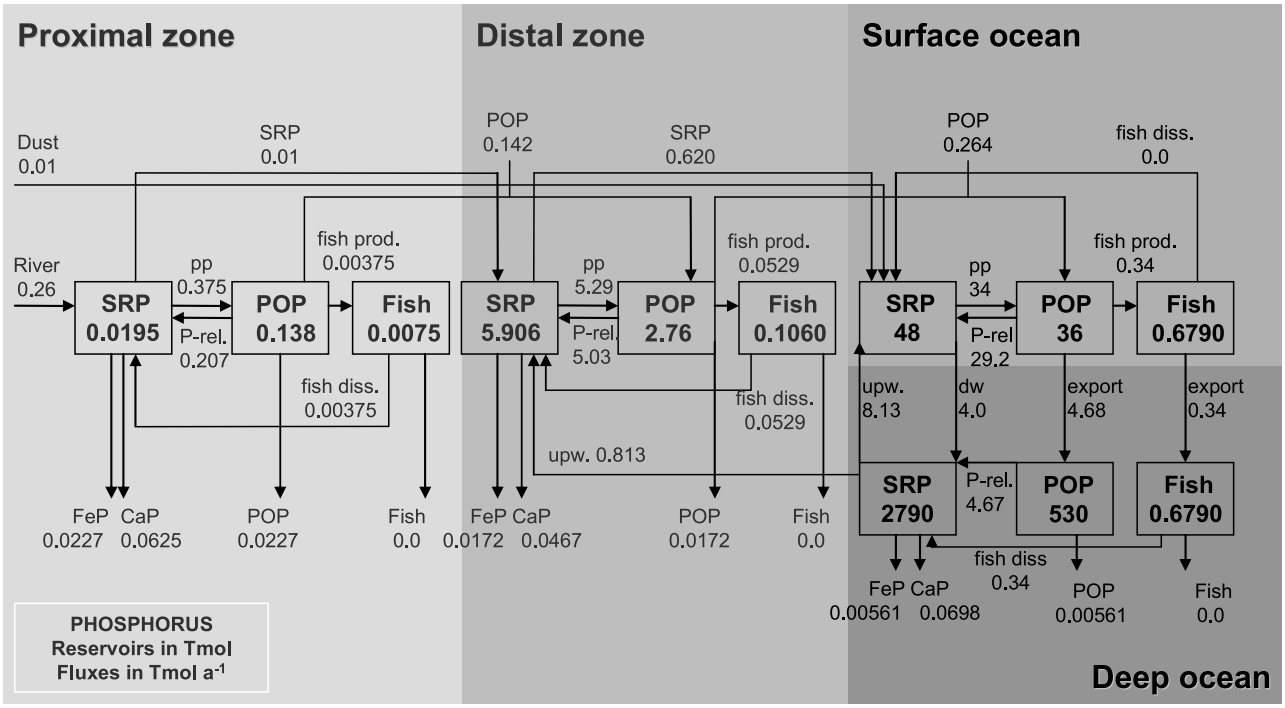

Figure 1. Preindustrial steady state phosphorus cycle implemented in the model. The model incorporates three phosphorus species: soluble reactive phosphorus (SRP), particulate organic phosphorus (POP), and fish hard parts (fish). Four oceanic zones are represented: the proximal zone, directly influenced by river input, the distal zone (average water depth 130 m), the mixed layer of the surface ocean (average depth 150 m), and deep ocean water. The values given are for a 13 ka residence time. The corresponding reservoir and flux values for a 39 ka residence time of reactive P in the oceans are given by *Slomp and Van Cappellen* [2007].

duction and increases both the burial of organic carbon and reactive phosphorus in deep-sea sediments. Thus, increased open ocean productivity during glacial times does not require enhanced chemical weathering on the continents.

[29] Upon sea level rise (interglacial stage), the reflooding of the coast increases the retention capacity of the coast again, and higher amounts of reactive P and organic C get buried there. This reduces the export of P to the open ocean, lowers surface ocean productivity, and organic matter export, thereby reoxygenating the oceanic water column.

3.3.2. Sensitivity to Mixing, Weathering, and Dust

[30] Because the changes in circulation, weathering, and eolian input over a full glacial-interglacial cycle are more poorly constrained than sea level, we look at the system sensitivity to a wide range of these forcings. The transient effects of changes in mixing and reactive P input through

Table 2. Comparison of Reservoir Masses and Fluxes of the Organic Carbon Cycle for a 39 ka P Residence Time Model and a 13 ka Residence Time Model[a]

	39 ka Model	39 ka Model[b]	13 ka Model
	Reservoirs (Tmol)		
C1: POC proximal coastal zone	4.5	3.5	14.7
	Fluxes (Tmol/a)		
CF2: POC mineralization in proximal zone	31.5	32.6	17.9
CF3: proximal sediment POC burial	3.6	3.6	6.8
CF4: POC export from proximal to distal zone	4.7	3.6	15
CF6: POC mineralization in distal zone	534	533	542
CF7: distal sediment POC burial	2.7	2.7	5.2
CF10: POC mineralization in surface ocean	3131	3131	3132
CF11: POC export from surface to deep ocean	497	497	496
CF13: deep-sea sediment POC burial	1.6	1.6	1.33

[a]Only modified reservoirs and fluxes are listed here; all other values are as specified by *Slomp and Van Cappellen* [2007]. The 39 ka P residence time model is given by *Slomp and Van Cappellen* [2007], and the 13 ka residence time model is given by this work. POC = particulate organic carbon.
[b]Modified for dust flux.

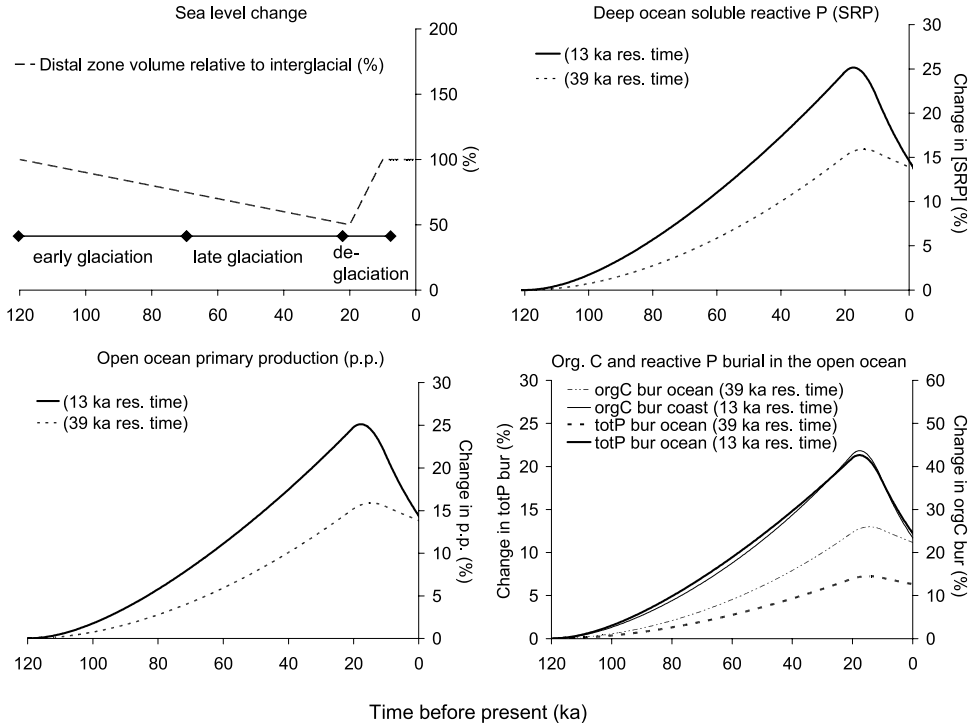

Figure 2. Model response to sea level change implemented as distal zone volume change: deep ocean soluble reactive phosphorus (SRP), oceanic primary production, organic carbon burial, and reactive P burial. All responses are plotted as percent change relative to interglacial values.

rivers and dust, over a glacial-interglacial cycle, are summarized in Figure 3. As changes in the deep ocean reservoirs and burial rates closely follow primary production (as illustrated in Figure 2), only open ocean primary production trends are shown. The sensitivity analysis is performed on the 13 ka residence time version of the model; as it is the more responsive of the two versions, it gives the upper bound of sensitivity.

[31] A 30% reduction in oceanic mixing strength for most of the glacial period (110,000–20,000 years B.P.) raises coastal productivity by 8% and decreases open ocean productivity by 15%. As such, these effects are smaller than those accompanying sea level fall. In fact, for mixing to affect primary production to the same extent as sea level change, a 50% reduction in vertical mixing would be necessary. Compared to oceanic upwelling, the effect of coastal upwelling is negligible (Figure 3).

[32] Decreasing the reactive P input from rivers reduces primary production both in the coastal zone and in the open ocean. Our glacial scenario of a 10% reduction in riverine input reduces primary production by <10% in both marine compartments. As such, weathering has a more limited effect than sea level. However, if the supply of reactive P were to decrease by 50% it could reverse the sea level effect on open ocean productivity and more than double the sea level effect in the coastal zone. In such a case, total marine productivity would decrease. An accurate chemical weathering scenario is therefore paramount for a meaningful assessment of the biogeochemistry of the oceans during glacial-interglacial transitions.

[33] Increasing the reactive P input from dust to the surface ocean stimulates primary production, but the scale of this effect is very small for the specified glacial scenario. There would have to be an order of magnitude increase in the dust supplied to the surface of the ocean for the effect of dust to be comparable to those inferred for sea level, mixing, and weathering. Doubling the reactive P input from dust boosts primary production only by 3–4%. Therefore, reactive P input via dust likely plays only a marginal role in the P cycle over glacial times.

[34] On the basis of the sensitivity tests outlined above, sea level and oceanic mixing emerge as the critical climatic parameters. Weathering is also a potentially important forcing if varied significantly; however, coastal upwelling and dust have relatively negligible effects on the system relative to the other forcings.

3.4. Model Implementation of Glacial-Interglacial Scenario

[35] The baseline glacial-interglacial scenario, based on the literature review outlined in section 2, accounts for the simultaneous variations in the major forcings on the marine P cycle: sea level, mixing, continental input of P, and sea surface temperature (Figure 4). Sea level is implemented in the model by reducing the distal coastal zone volume linearly by 50% (see Figure 2) over 100 ka during glaciation and reincreasing it over 10 ka during deglaciation. The proximal coastal zone is assumed to move along the coast but its size remains the same. In the baseline scenario, the river input of reactive phosphorus is reduced linearly start-

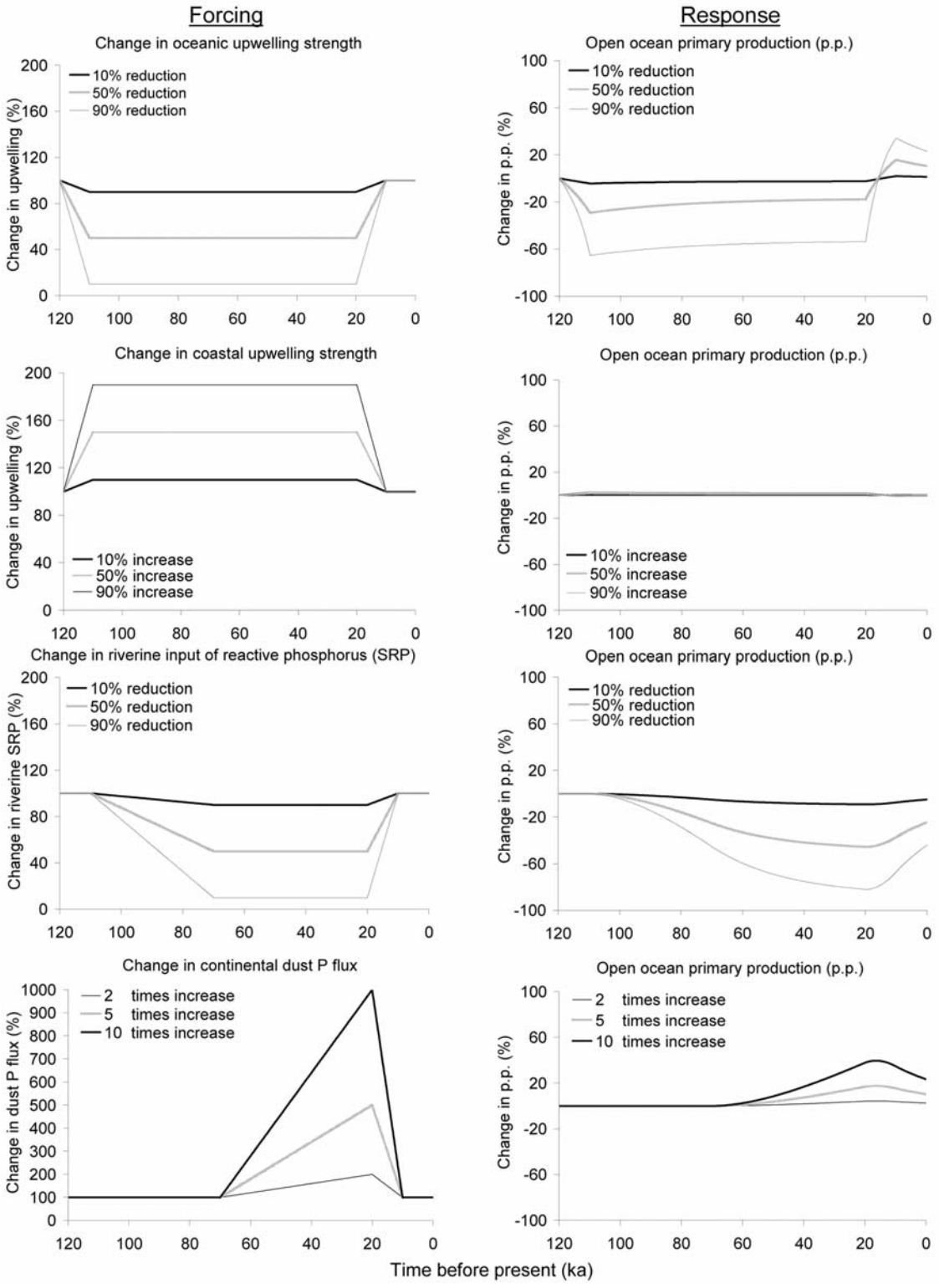

Figure 3. Sensitivity of primary production to changes in circulation (open ocean and coastal upwelling), nutrient loading from the continents, and dust input. The results shown are for the 13 ka residence time version of the model; the 39 ka residence time version behaves in the same way but with a longer time lag. All values are given as percent change relative to interglacial.

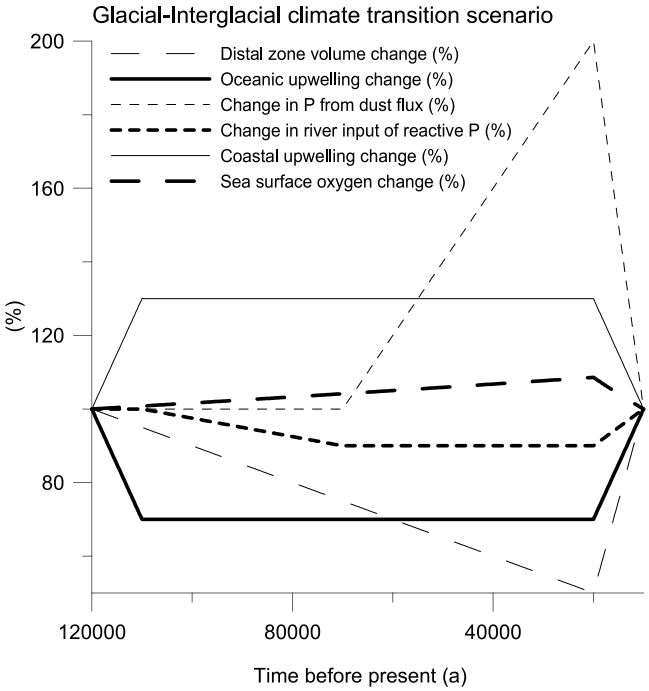

Figure 4. Glacial-interglacial scenario implemented in the box model. All parameters are plotted as percent change relative to interglacial values. During 100 ka of glaciation the distal zone volume decreases to 50% of the starting value and returns linearly to the starting value during deglaciation. During the first 10 ka of glaciation, coastal upwelling increases by 30% and oceanic upwelling decreases by 30%. During deglaciation they return to starting values. During the first 50 ka of glaciation, continental input of reactive P decreases by 10% and returns to starting values during deglaciation. Dust supplied reactive P increases twofold during the last 50 ka of glaciation and returns to starting values upon deglaciation.

ing at 110 ka before present (B.P.) until 70 ka B.P., when the weathering reaches 90% of the interglacial value and remains that way until deglaciation, when it increases linearly back to the interglacial value. The eolian reactive P input to the surface of the open ocean increases linearly, from 70 ka B.P., until the LGM where the flux is double the interglacial value. The dust flux then returns linearly down to its initial value during deglaciation. We also implement the effect of a linear 4°C cooling during glaciation on O_2 solubility in surface waters according to *Pilson* [1998].

[36] Circulation is represented in the model through an open ocean upwelling flux (vertical mixing in the ocean) and a coastal upwelling flux (oceanic deep water export to the coast). To change the upwelling rates, these fluxes are multiplied by a scaling factor. For the proposed baseline scenario, we impose a 30% decrease in oceanic upwelling during early glaciation (first 10 ka) and a return to full-strength mixing (over 10 ka) during deglaciation. On the basis of the work of *Slomp and Van Cappellen* [2007], the coastal upwelling term has only a negligible effect on the oceanic P reservoirs, and thus a strict constraint on coastal upwelling intensity is not necessary. We simply vary the coastal upwelling flux antisymetrically to the oceanic upwelling flux, i.e., coastal upwelling is increased by the same amount as oceanic upwelling is decreased.

3.5. Model Spin-Up

[37] Given the timescales of glacial-interglacial transitions (~100 ka for glaciations, ~10 ka for deglaciations), the marine P cycle could not have been at steady state during the repeated glacial-interglacial climate change characterizing the Quaternary, a concern raised previously by *Wallmann* [2003]. Applying consecutive glacial-interglacial perturbations shows (Figure 5) that the system response during the first cycle is markedly different from subsequent responses. Under the applied periodic forcings, the system quickly shifts to an oscillatory mode exhibiting repetitive patterns (Figure 5). We therefore applied a spin-up procedure, detailed below and illustrated in Figure 5, to allow the system to equilibrate with the imposed forcings.

[38] Once the system is equilibrated with the cyclical forcings, the initial conditions of the model are offset so that the constraints on the interglacial marine P cycle (sections 3.1 and 3.2) are met for the equilibrated state of the system, rather than imposed as starting values. The constraints are assumed to be representative for the last interglacial (10 ka B.P.). This shift in initial conditions (starting values of reservoirs and fluxes) is applied until all reservoirs and fluxes specified in Figure 1 and Table 2 are satisfied for an equilibrated interglacial state (e.g., see Figure 5 for SRP and primary production examples).

[39] The two residence time versions of the model show similar qualitative behavior but differ in the degree of departure between the initial and equilibrated state, as well as the equilibration time. The longer residence time model (39 ka) moves further away from its initial conditions and requires seven glacial-interglacial cycles to equilibrate with the forcings (equilibration is reached when the system returns to the same interglacial state at the end of a cycle), while the 13 ka residence time model only requires four glacial-interglacial cycles to equilibrate (Figure 5).

4. Results and Discussion: Glacial-Interglacial Transition Scenario

[40] The main objective of our simulations is to determine how primary production and burial of organic carbon and reactive phosphorus respond to the combined changes in the environmental forcings identified above (Figure 4).

[41] The results of the complete glacial-interglacial scenario, as detailed in section 3, are shown in Figures 6 and 7. The model outcomes, namely deep ocean SRP, primary production, organic C burial, and reactive P burial, roughly follow the trends induced by sea level change (compare with Figure 2), with some notable differences. First, oceanic primary production and organic C and P burial decrease at the beginning of glaciation, before increasing again toward the LGM. Second, there is a temporal offset with respect to the LGM: primary production, organic carbon C, and P burial all peak during the postglacial (interglacial) period. Thus, while sea level change emerges as a dominant

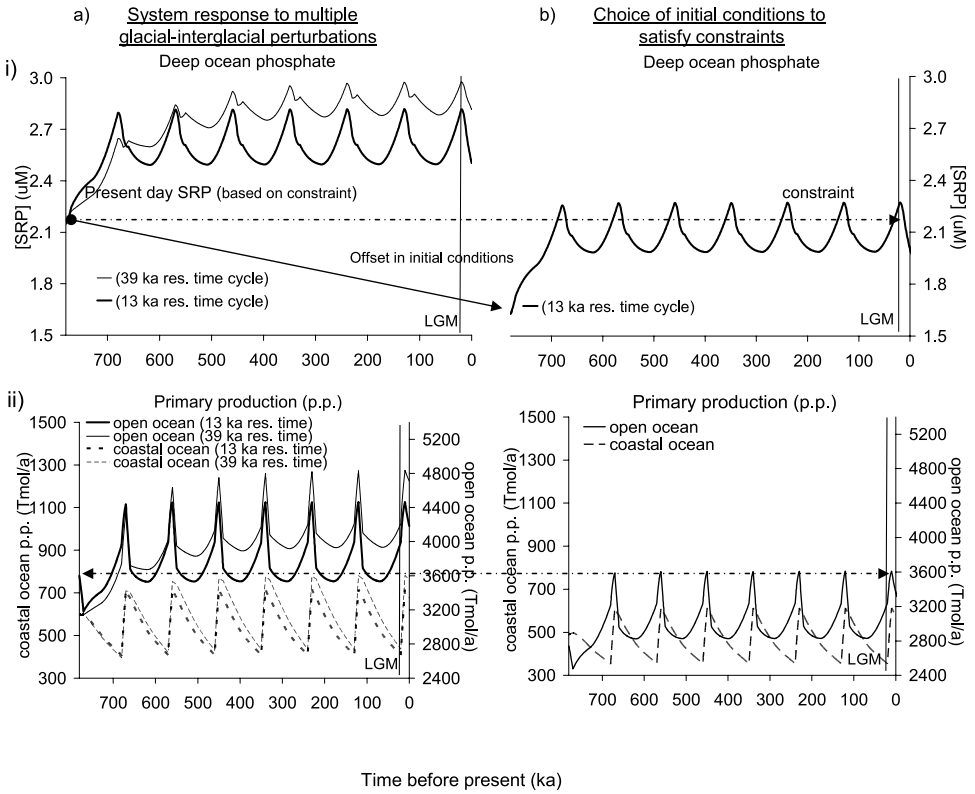

Figure 5. Model spin-up. Model response (soluble reactive P and primary production) to consecutive glacial-interglacial perturbations. (a) On the basis of an initial steady state, the system (both 13 ka and 39 ka version) is allowed to evolve under periodic perturbations. (b) The initial conditions are adjusted so that model constraints are met at the last interglacial (10 ka B.P.). The spin-up is applied to the 13 ka residence time version of the model only.

forcing, it cannot alone describe the full glacial-interglacial scenario. On the basis of the sensitivity results, mixing and weathering act as important secondary forcings, counterbalancing and distorting the trends due to sea level.

[42] During glaciation, soluble reactive phosphorus is gradually transferred to the open ocean; the deep ocean SRP inventory increases by 5%, relative to its interglacial value, at the LGM. Open ocean productivity initially drops, due to the slower mixing sequestering reactive P in the deep ocean, but, as the deep ocean P inventory increases, primary production increases again. It is noteworthy, however, that primary production during glacial time is shown to be lower than during interglacial periods. Coastal production decreases by 40% over the glacial period. Organic carbon burial follows the productivity trends with a 20% decrease in deep-sea burial during glaciation and a concurrent 25% decrease in coastal areas.

[43] During deglaciation the reactive P inventory of the deep ocean returns to its starting value. However, due to enhanced vertical mixing, more reactive P is supplied to surface waters. As a result, oceanic production continues to increase until it peaks at 10 ka B.P. This is due to enhanced weathering and mixing counteracting the effect of rising sea level.

[44] Deep water oxygen initially decreases during glaciation (due to slowdown in mixing) but increases in the middle and late glaciation. Waters are oxygenated then because the effect of reduced mixing is gradually overtaken by sea surface cooling bringing in more dissolved oxygen from surface waters. Deep water oxygen does not fall much during the glacial cycle. Although additional mechanisms can affect the deep-sea O_2 level, the estimated variations in deep-sea oxygenation should have a negligible effect on the primary production linked to redox-dependent P regeneration.

[45] In the deep ocean, iron-bound phosphorus burial is highest during the period when deep-sea O_2 levels are highest. Thus, the iron-bound P fraction is high during glaciation and lower during interglacial periods. The burial of the other reactive P phases (CaP, POP), on the other hand, increases during interglacials (see Figure 7). Because FeP is a very small fraction of total reactive P, the net effect is one of a 10% decrease of reactive P preservation in deep-sea sediments during the LGM. The role of coastal sediments in removing reactive P also decreases during glaciation. Burial of all P phases (CaP, FeP, POP) drops by approximately 13% in the coastal zone. Integrated over the coastal and open ocean, one glacial-interglacial perturbation has the effect of lowering total reactive P burial by 20%, thereby increasing the residence time of P in the ocean.

[46] While the reactive P inventory of the ocean peaks during the LGM, primary production is lower throughout

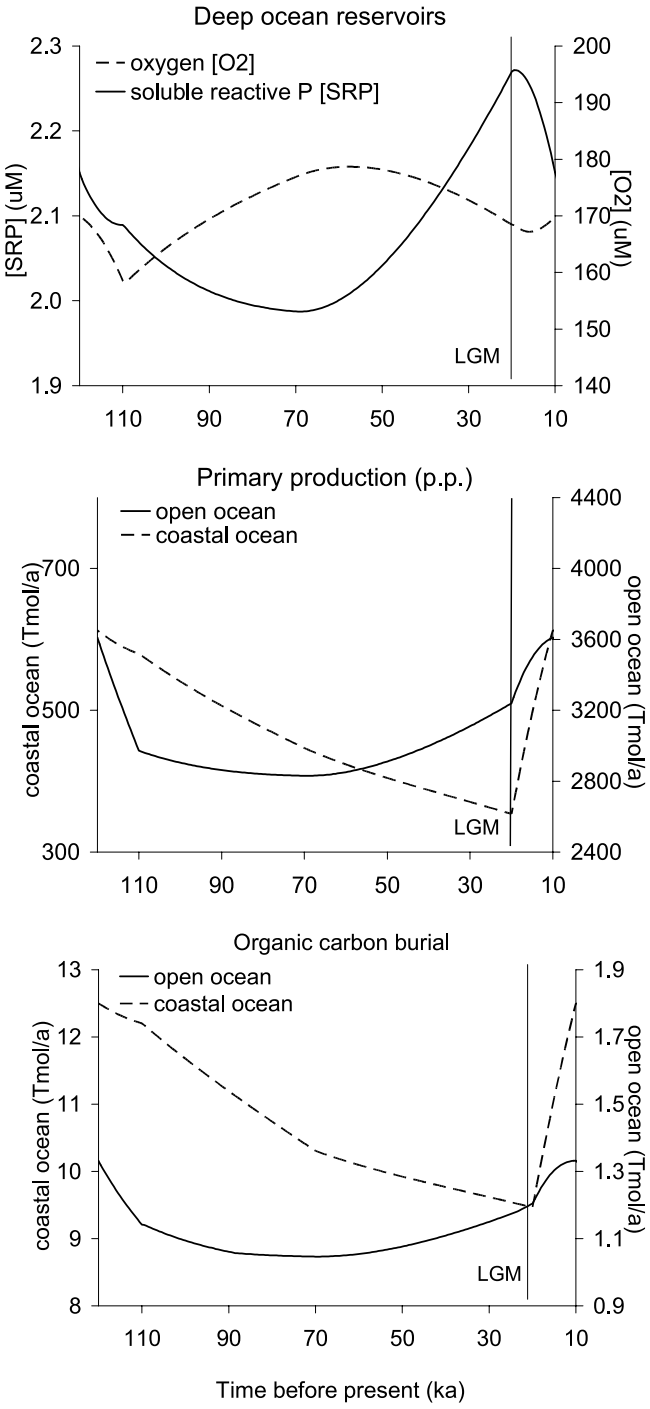

Figure 6. Model response to combined glacial scenario of sea level, circulation, weathering, and dust flux changes: deep-sea oxygen concentration [O_2] and soluble reactive P (SRP), primary production (p.p.), and organic carbon burial in the open ocean and coastal ocean (13 ka model after spin-up).

glacial times, it increases during postglacial periods, and is maximum at the end of interglacials. Similarly, the burial of P in the ocean does not increase during glaciation but decreases and then gradually returns to its interglacial value. These results therefore do not support our starting hypothesis of an enhancement in primary production due to changes in the marine P cycle during the glacial period. Therefore, the response of the marine P cycle to the imposed set of forcings does not, in itself, contribute to the drawdown of atmospheric CO_2 during glaciation.

5. Comparison to Paleo-Evidence

[47] As far as reactive P and organic C behavior during glacial times is concerned, there is supporting evidence in the geological record for the predictions of the model. Model results show reactive P in deep ocean waters peaking during glacial maxima (0.13 μM higher than at interglacial). *Elderfield and Rickaby* [2000] find the PO_4 inventory not significantly different in the subantarctic regions but up by 0.6 μM in the Antarctic. Increase in the oceanic phosphate reservoir during glaciation has been proposed earlier and, while reports on the glacial deep water phosphate are sparse, estimates range up to 3.2 μM [*Broecker*, 1982] compared to our result of 2.3 μM at the LGM.

[48] In a global study, *Kohfeld et al.* [2005] propose that throughout most of the world's oceans, primary production decreased at the beginning of glaciation (until stage 5a-d, ending approximately 80 ka B.P.) and subsequently increased. This is in line with our model results which show a dip in primary production until approximately 70 ka B.P. followed by an increase, returning to interglacial values (Figure 6). In contrast, *Mix* [1989] and *Sarnthein et al.* [1988] report a higher primary production (28–80%) for the Atlantic at the LGM. However, in most current high production areas, new production at the LGM was higher, with peak production at approximately 15 ka B.P. (the interglacial period); in modern low production zones, glacial productivity did not vary systematically. Similar evidence was found by *Pedersen* [1983] in the eastern equatorial Pacific for a peak in surface ocean production at 15–14 ka B.P. *Filippelli et al.* [2007] report higher primary production toward the end of glacials and the beginning of interglacials for sites in the Southern and equatorial Pacific oceans. *Romero et al.* [2006] also report continued surface water productivity enhancement after the LGM into the Holocene, off the coast of Chile.

[49] Organic carbon burial in our model follows the trends of primary production. Organic carbon burial in the open ocean increases during the late glacial and peaks during the interglacial period. *Broecker* [1982] summarizes corroborating evidence which points to a peak in organic carbon burial after the glacial maximum. We also find that oceanic P burial is higher after the LGM than during glaciation. *Tamburini* [2001] reports a similar trend in the average standardized P mass accumulation rates (MAR) of eight deep-sea cores: there is an initial decrease in P burial until approximately 75 ka B.P. followed by a gradual increase back to starting values at approximately 10 ka B.P. Although a quantitative comparison cannot be made, our model results also show a decrease in P burial until approximately 70 ka B.P. followed by an increase and return to interglacial values. Overall, keeping in mind the heterogeneity of the ocean system, our model results tend to

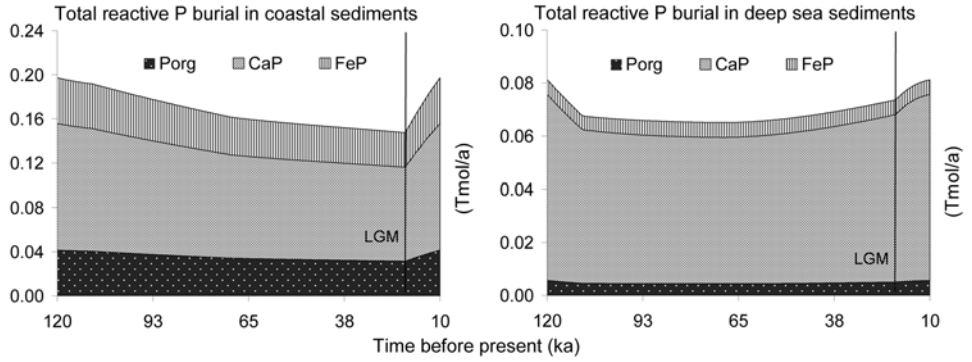

Figure 7. Model response to combined glacial scenario of sea level, circulation, weathering, and dust flux changes continued. Reactive phosphorus burial: iron-bound phosphorus (FeP), calcium-associated authigenic phosphorus (CaP), and organic phosphorus (Porg).

agree with the general glacial period constraints based on paleoceanographic evidence for the last glacial-interglacial cycle.

6. Conclusions and Implications

[50] The model results illustrate that the marine P cycle is sensitive to climate-related variations accompanying glacial-interglacial cycles. The importance of individual forcings on the marine P cycle changes during the glacial-interglacial transition (Table 3). During early glaciation (120–70 ka B.P.), oceanic mixing has a dominant effect, because of the rapid change in overturning and the high sensitivity of the marine P cycles to that parameter. Primary production and associated burial of organic C and reactive P all fall because of the slowdown in nutrient redistribution to the surface ocean. During late glaciation (70–20 ka B.P.), however, the cumulative effect of sea level fall on the coastal shelves becomes the prominent forcing. As the coastal filter shrinks, effective transport of nutrients to the open ocean helps restore primary production and burial fluxes. Deglaciation (20–10 ka B.P.), in turn, experiences the opposing effects of sea level rise and circulation (and weathering) increase. The net effect is one of enhanced primary production due to enhanced mixing and supply of nutrients, despite the increased ability of the coastal regions to retain reactive P. Our results augment the conclusions of *Wallmann* [2003], who focused primarily on the role of sea level change, by showing that the trend in marine P cycling is not one of sea level change alone but other forcings have complementary effects on the system.

[51] The assumed residence times of marine P (13 ka and 39 ka) do not qualitatively affect the P cycle's response to the imposed forcings, in particular the temporal change in primary production (Figure 5). There is a net enhancement of the deep ocean phosphate inventory during a glacial cycle. Despite the enhanced dissolved P inventory, however, primary production is lower during glaciation than during interglacial periods. Similarly, organic C and reactive P burial are lower during glacial times, increasing the residence time of P in the oceans.

[52] These findings are significant for the debate over the role of the biological pump in CO_2 sequestration during glaciations. Our results show that the biological pump may in fact have been weaker during glacial periods relative to interglacials. Thus, variations in the marine P cycle cannot be a contributing mechanism to the cyclical CO_2 drawdown trend, as production is lower at times when CO_2 drawdown should increase. In any event, given the magnitude of model-predicted fluctuations in the primary production, variation in the latter should be negligible compared to physical effects such as the sea surface temperature effect on CO_2 solubility or CO_2 sequestration due to circulation slowdown.

[53] Our model does not capture the effects of wind regimes and temperature on circulation nor other spatially variable effects on mixing intensities and oceanic P cycling. Also, the results of the present model reflect the trend of the average (total ocean average) rather than the average of the trend. The realism of the results reported above could be further improved by subdividing the ocean in a larger number of boxes, for example, by including separate high

Table 3. Timeline of Marine P Cycle Response to Glacial-Interglacial Transition

Period	Time	Response	Dominant Forcing(s)
Early glaciation	120–70 ka B.P.	primary production, organic C, and reactive P burial decrease	circulation slowdown
Late glaciation	70–20 ka B.P.	reactive P is transported to the open ocean	sea level fall
Deglaciation	20–10 ka B.P.	primary production, organic C, and reactive P burial increase more P retained in the coastal ocean primary production, organic C, and reactive P burial increase toward their maximum values	enhanced circulation and weathering

latitude boxes, and by implementing a more dynamic modulation of the exchange of waters between the surface and the deep ocean. Also, a logical next step is the inclusion of a more elaborate description of the P cycle in a biogeochemical ocean general circulation model (GCM).

[54] As yet, available GCMs do not include a separate representation of the continental margins. This makes box models such as ours indispensable tools to assess and untangle the combined effects of sea level change and various climate forcings on the coupled P and C cycles. Our model allows us to show that sea level is likely not the only relevant forcing during glaciation and that during different periods of a glacial-interglacial cycle other climate variables (such as mixing and nutrient supply) gain importance. We also find counterintuitive results, such as a lowering of primary production during glacial times, contradicting the biological pump theory.

[55] **Acknowledgments.** This research was made possible by financial support from the Netherlands Organisation for Scientific Research (VIDI grant to C.P. Slomp) and Utrecht University (HiPo project G-NUX to C.P. Slomp).

References

An, Z. S., G. Kukla, S. C. Porter, and J. L. Xiao (1991), Late Quaternary dust flow on the Chinese loess plateau, *Catena*, *18*, 125–132, doi:10.1016/0341-8162(91)90012-M.

Anderson, L. D., M. L. Delaney, and K. L. Faul (2001), Carbon to phosphorus ratios in sediments: Implications for nutrient cycling, *Global Biogeochem. Cycles*, *15*, 65–79, doi:10.1029/2000GB001270.

Anderson, R. F., M. Q. Fleisher, and Y. Lao (2006), Glacial–interglacial variability in the delivery of dust to the central equatorial Pacific Ocean, *Earth Planet. Sci. Lett.*, *242*, 406–414, doi:10.1016/j.epsl.2005.11.061.

Archer, D., A. Winguth, D. Lea, and N. Mahowald (2000a), What caused the glacial/interglacial atmospheric pCO_2 cycles?, *Rev. Geophys.*, *38*, 159–189, doi:10.1029/1999RG000066.

Archer, D. E., G. Eshel, A. Winguth, W. Broecker, R. Pierrehumbert, M. Tobis, and R. Jacob (2000b), Atmospheric pCO_2 sensitivity to the biological pump in the ocean, *Global Biogeochem. Cycles*, *14*, 1219–1230, doi:10.1029/1999GB001216.

Benitez-Nelson, C. R. (2000), The biogeochemical cycling of phosphorus in marine systems, *Earth Sci. Rev.*, *51*, 109–135, doi:10.1016/S0012-8252(00)00018-0.

Bigg, G. R., M. R. Wadley, D. P. Stevens, and J. A. Johnson (1998), Simulations of two Last Glacial Maximum ocean states, *Paleoceanography*, *13*, 340–351, doi:10.1029/98PA00402.

Boyd, P. W., and T. W. Trull (2007), Understanding the export of biogenic particles in oceanic waters: Is there consensus?, *Prog. Oceanogr.*, *72*, 276–312, doi:10.1016/j.pocean.2006.10.007.

Broecker, W. S. (1982), Ocean chemistry during glacial time, *Geochim. Cosmochim. Acta*, *46*, 1689–1705, doi:10.1016/0016-7037(82)90110-7.

Broecker, W. S. (1987), Palaeoocean circulation rates as determined from radiocarbon measurements on hand-picked foraminifera, *Terra Cognita*, *7*, 43–44.

Broecker, W. S. (1997), Thermohaline circulation, the Achilles Heel of our climate system: Will man-made CO_2 upset the current balance?, *Science*, *278*, 1582–1588, doi:10.1126/science.278.5343.1582.

Broecker, W. S., and G. M. Henderson (1998), The sequence of events surrounding Termination II and their implications for the cause of glacial-interglacial CO_2 changes, *Paleoceanography*, *13*, 352–364, doi:10.1029/98PA00920.

Broecker, W. S., S. Barker, E. Clark, I. Hajdas, G. Bonani, and S. Lowell (2004), Ventilation of the glacial deep Pacific Ocean, *Science*, *306*, 1169–1172, doi:10.1126/science.1102293.

Christensen, J. P. (1994), Carbon export from continental shelves, denitrification and atmospheric carbon dioxide, *Cont. Shelf Res.*, *14*, 547–576, doi:10.1016/0278-4343(94)90103-1.

CLIMAP Project Members (1981), Seasonal reconstructions of the Earth's surface at the Last Glacial Maximum, *Geol. Soc. Am. Map Chart Ser.*, *36*, Geol. Soc. of Am., Boulder, Colo.

Compton, J., D. Mallinson, C. R. Glenn, G. Filippelli, K. Föllmi, G. Shields, and Y. Zanin (2000), Variations in the global phosphorus cycle, in *Marine Authigenesis: From Global to Microbial*, *Spec. Publ. SEPM Soc. Sediment. Geol.*, *66*, 21–33.

Corliss, B. H., D. G. Martinson, and T. Keffer (1986), Late Quaternary deep-ocean circulation, *Geol. Soc. Am. Bull.*, *97*, 1106–1121, doi:10.1130/0016-7606(1986)97<1106:LQDC>2.0.CO;2.

De La Rocha, C. L., and U. Passow (2007), Factors influencing the sinking of POC and the efficiency of the biological carbon pump, *Deep Sea Res., Part II*, *54*, 639–658, doi:10.1016/j.dsr2.2007.01.004.

Delmonte, B., I. Basile-Doelsch, J.-R. Petit, V. Maggi, M. Revel-Rolland, A. Michard, E. Jargoutz, and F. Grousset (2004), Comparing the Epica and Vostok dust records during the last 220,000 years: Stratigraphical correlation and provenance in glacial periods, *Earth Sci. Rev.*, *66*, 63–87, doi:10.1016/j.earscirev.2003.10.004.

Deutsch, C., D. M. Sigman, R. C. Thunell, A. N. Meckler, and G. H. Haug (2004), Isotopic constraints on glacial/interglacial changes in the oceanic nitrogen budget, *Global Biogeochem. Cycles*, *18*, GB4012, doi:10.1029/2003GB002189.

Elderfield, H., and R. E. M. Rickaby (2000), Oceanic Cd/P ratio and nutrient utilization in the glacial Southern Ocean, *Nature*, *405*, 305–310, doi:10.1038/35012507.

Fairbanks, R. G. (1989), A 17,000 glacio-eustatic sea level record: Influence of glacial melting rates on the Younger Dryas event and deep circulation, *Nature*, *342*, 637–642, doi:10.1038/342637a0.

Falkowski, P. G. (1997), Evolution of the nitrogen cycle and its influence on the biological sequestration of CO_2 in the ocean, *Nature*, *387*, 272–275, doi:10.1038/387272a0.

Filippelli, G. M. (2002), The global marine phosphorus cycle, *Rev. Mineral. Geochem.*, *48*, 391–425.

Filippelli, G. M., J. C. Latimer, R. W. Murray, and J. A. Flores (2007), Productivity records from the Southern Ocean and the equatorial Pacific Ocean: Testing the glacial shelf-nutrient hypothesis, *Deep Sea Res., Part II*, *54*, 2443–2452, doi:10.1016/j.dsr2.2007.07.021.

Föllmi, K. B. (1995), 160 m.y. record of marine sedimentary phosphorus burial: Coupling of climate and continental weathering under greenhouse and icehouse conditions, *Geology*, *23*, 859–862, doi:10.1130/0091-7613(1995)023<0859:MYROMS>2.3.CO;2.

François, R., M. A. Altabet, E.-F. Yu, D. M. Sigman, M. P. Bacon, M. Frank, G. Bohrmann, G. Bareille, and L. D. Labeyrie (1997), Contribution of Southern Ocean surface-water stratification to low atmospheric CO_2 concentrations during the last glacial period, *Nature*, *389*, 929–935, doi:10.1038/40073.

Froelich, P. N., M. L. Bender, N. A. Luedtke, G. R. Heath, and T. DeVries (1982), The marine phosphorus cycle, *Am. J. Sci.*, *282*, 474–511.

Ganopolski, A., S. Rahmstorf, V. Petoukhov, and M. Claussen (1998), Simulation of modern and glacial climates with a coupled global model of intermediate complexity, *Nature*, *391*, 351–356, doi:10.1038/34839.

Graham, W. F., and R. A. Duce (1982), The atmospheric transport of phosphorus to the western North Atlantic, *Atmos. Environ.*, *16*, 1089–1097, doi:10.1016/0004-6981(82)90198-6.

Harrison, S. P., K. E. Kohfeld, C. Roelandt, and T. Claquin (2001), The role of dust in climate changes today, at the Last Glacial Maximum and in the future, *Earth Sci. Rev.*, *54*, 43–80, doi:10.1016/S0012-8252(01)00041-1.

Hay, W., and J. R. Southam (1977), Modulation of marine sedimentation by the continental shelves, in *Marine Science 6: The Fate of Fossil Fuel CO_2 in the Oceans*, edited by N. R. Andersen and A. Malahoff, pp. 572–604, Plenum Press, New York.

Hedges, J. I., and R. G. Keil (1995), Sedimentary organic matter preservation: An assessment and speculative synthesis, *Mar. Chem.*, *49*, 81–115, doi:10.1016/0304-4203(95)00008-F.

Heinze, C., E. Maier-Reimer, A. Winguth, and D. Archer (1999), A global oceanic sediment model for long term climate studies, *Global Biogeochem. Cycles*, *13*, 221–250, doi:10.1029/98GB02812.

Hesse, P. P. (1994), The record of continental dust from Australia in Tasman Sea sediments, *Quat. Sci. Rev.*, *13*, 257–272, doi:10.1016/0277-3791(94)90029-9.

Holland, H. D. (1984), *The Chemical Evolution of the Atmosphere and Oceans*, 566 pp., John Wiley, New York.

Howarth, R. W., H. S. Jensen, R. Marino, and H. Postma (1995), Transport to and processing of P in near-shore and oceanic waters, in *Phosphorus in the Global Environment: Transfers, Cycles and Management, SCOPE*, 54, edited by H. Tiessen, pp. 323–345, John Wiley, New York.

Hughen, K., S. Lehman, J. Southon, J. Overbeck, O. Marchal, C. Herring, and J. Turnbull (2004), ^{14}C activity and global carbon cycle changes over the past 50,000 years, *Science*, *303*, 202–207, doi:10.1126/science.1090300.

Jaccard, S. L., G. H. Haug, D. M. Sigman, T. F. Pedersen, H. R. Thierstein, and U. Röhl (2005), Glacial/interglacial changes in subarctic north Pacific stratification, *Science*, *308*, 1003–1006, doi:10.1126/science.1108696.

Jewell, P. W. (1994), Mass balance models of Eckman transport and nutrient fluxes in coastal upwelling zones, *Global Biogeochem. Cycles*, *8*, 165–177, doi:10.1029/94GB00097.

Kageyama, M., et al. (2006), Last Glacial Maximum temperatures over the North Atlantic, Europe and western Siberia: A comparison between PMIP models, MARGO sea-surface temperatures and pollen-based reconstructions, *Quat. Sci. Rev.*, *25*, 2082–2102, doi:10.1016/j.quascirev.2006.02.010.

Keigwin, L. D. (1998), Glacial-age hydrography of the northwest Pacific Ocean, *Paleoceanography*, *13*, 323–339, doi:10.1029/98PA00874.

Kohfeld, K. E., and S. P. Harrison (2001), DIRTMAP: The geological record of dust, *Earth Sci. Rev.*, *54*, 81–114, doi:10.1016/S0012-8252(01)00042-3.

Kohfeld, K. E., C. LeQuere, S. P. Harrison, and R. F. Anderson (2005), Role of marine biology in glacial interglacial CO_2 cycles, *Science*, *308*, 74–78, doi:10.1126/science.1105375.

Köhler, P., and H. Fischer (2006), Proposing a mechanistic understanding of changes in atmospheric CO_2 during the last 740 000 years, *Clim. Past Disc.*, *2*, 1–42.

Kump, L. R., and R. B. Alley (1994), Global chemical weathering on glacial time scales, in *Material Fluxes on the Surface of the Earth*, pp. 46–60, Natl. Acad. Press, Washington, D. C.

Lambeck, K., and J. Chappell (2001), Sea Level change through the last glacial cycle, *Science*, *292*, 679–685, doi:10.1126/science.1059549.

Latimer, J. C., and G. M. Filippelli (2001), Terrigenous input and paleoproductivity in the Southern Ocean, *Paleoceanography*, *16*(6), 627–643, doi:10.1029/2000PA000586.

Latimer, J. C., G. M. Filippelli, I. Hendy, and D. R. Newkirk (2006), Opal-associated particulate phosphorus: Implications for the marine P cycle, *Geochim. Cosmochim. Acta*, *70*, 3843–3854, doi:10.1016/j.gca.2006.04.033.

Lefevre, N., and A. J. Watson (1999), Modeling the geochemical cycle of iron in the oceans and its impact on atmospheric CO_2 concentrations, *Global Biogeochem. Cycles*, *13*, 727–736, doi:10.1029/1999GB900034.

LeGrand, P., and C. Wunsch (1995), Constraints from paleotracer data on the North Atlantic circulation during the Last Glacial Maximum, *Paleoceanography*, *10*, 1011–1045, doi:10.1029/95PA01455.

LeGrand, M. R., C. Lorius, N. I. Barkov, and N. V. Petrov (1988), Vostok (Antarctica) ice core: Atmospheric chemistry changes over the last climactic cycle, *Atmos. Environ.*, *22*, 317–331, doi:10.1016/0004-6981(88)90037-6.

Lerman, A. (1994), Surficial weathering fluxes and their geochemical controls, in *Material Fluxes on the Surface of the Earth*, pp. 28–45, Natl. Acad. Press, Washington, D. C.

Ludwig, W., and J.-L. Probst (1999), Soil erosion and atmospheric CO_2 during the Last Glacial Maximum: The role of riverine organic matter fluxes, *Tellus, Ser. B*, *51*, 156–164.

Ludwig, W., P. Amiotte-Suchet, and J.-L. Probst (1999), Enhanced chemical weathering of rocks during the Last Glacial Maximum: A sink for atmospheric CO_2?, *Chem. Geol.*, *159*, 147–161, doi:10.1016/S0009-2541(99)00038-8.

Lyle, M. W., F. G. Prahl, and M. A. Sparrow (1992), Upwelling and productivity changes inferred from a temperature record in the central equatorial Pacific, *Nature*, *355*, 812–815, doi:10.1038/355812a0.

Lynch-Stieglitz, J., W. B. Curry, and N. Slowey (1999), Weaker Gulf stream in the Florida straits during the Last Glacial Maximum, *Nature*, *402*, 644–648, doi:10.1038/45204.

Marchal, O., R. François, T. F. Stocker, and F. Joos (2000), Ocean thermohaline circulation and sedimentary $^{231}Pa/^{230}Th$ ratio, *Paleoceanography*, *15*, 625–641, doi:10.1029/2000PA000496.

Martinez, P., P. Bertrand, G. B. Shimmield, K. Cochrane, F. J. Jorissen, J. Foster, and M. Digman (1999), Upwelling intensity and ocean productivity changes off Cape Blanc (northwest Africa) during the last 70,000 years: Geochemical and micropalaentological evidence, *Mar. Geol.*, *158*, 57–74, doi:10.1016/S0025-3227(98)00161-3.

McManus, J. F., D. W. Oppo, and J. L. Cullen (1999), A 0.5-million-year record of millennial-scale climate variability in the North Atlantic, *Science*, *283*, 971–975.

Meissner, K. J., A. Schmittner, A. J. Weaver, and J. F. Adkins (2003), Ventilation of the North Atlantic Ocean during the Last Glacial Maximum: A comparison between simulated and observed radiocarbon ages, *Paleoceanography*, *18*(2), 1023, doi:10.1029/2002PA000762.

Mix, A. C. (1989), Influence of productivity variations on long term atmospheric CO_2, *Nature*, *337*, 541–544, doi:10.1038/337541a0.

Paul, A., and C. Schäfer-Neth (2003), Modeling the water masses of the Atlantic Ocean at the Last Glacial Maximum, *Paleoceanography*, *18*(3), 1058, doi:10.1029/2002PA000783.

Peacock, S., E. Lane, and J. M. Restrepo (2006), A possible sequence of events for the generalized glacial-interglacial cycle, *Global Biogeochem. Cycles*, *20*, GB2010, doi:10.1029/2005GB002448.

Pedersen, T. F. (1983), Increased productivity in the eastern equatorial Pacific during the Last Glacial Maximum (19,000 to 14,000 yr B.P.), *Geology*, *11*, 16–19, doi:10.1130/0091-7613(1983)11<16:IPITEE>2.0.CO;2.

Peltier, W. R. (1994), Ice age paleotopography, *Science*, *265*, 195–201, doi:10.1126/science.265.5169.195.

Petit, C., et al. (1999), Climate and atmospheric history of the past 420,000 years from the Vostok ice core, Antarctica, *Nature*, *399*, 429–436, doi:10.1038/20859.

Pilson, M. E. Q. (1998), *An Introduction to the Chemistry of the Sea*, 389 pp., Prentice Hall, N. J.

Rahmstorf, S. (2002), Ocean circulation and climate during the past 120,000 years, *Nature*, *419*, 207–214, doi:10.1038/nature01090.

Rea, D. K., S. A. Hovan, and T. R. Janecek (1994), Late Quaternary flux of eolian dust to the Pelagic Ocean, in *Material Fluxes on the surface of the Earth*, pp. 116–124, Natl. Acad. Press, Washington, D. C.

Ridgwell, A. J. (2001), Glacial-interglacial perturbations in the global carbon cycle, Ph.D. thesis, 137 pp., Univ. of East Anglia, Norwich, UK.

Ridgwell, A. J. (2003), Implications of the glacial CO_2 "iron hypothesis" for Quaternary climate change, *Geochem. Geophys. Geosyst.*, *4*(9), 1076, doi:10.1029/2003GC000563.

Romero, O., G. Mollenhauer, R. R. Schneider, and G. Wefer (2003), Oscillations of the siliceous imprint in the central Benguela Upwelling System from MIS 3 through the early Holocene: The influence of the Southern Ocean, *J. Quat. Sci.*, *18*, 733–743, doi:10.1002/jqs.789.

Romero, O. E., J.-H. Kim, and D. Hebbeln (2006), Paleoproductivity evolution off central Chile from the Last Glacial Maximum to the early Holocene, *Quat. Res.*, *65*, 519–525, doi:10.1016/j.yqres.2005.07.003.

Rutberg, R. L., and S. L. Peacock (2006), High-latitude forcing of interior ocean $\delta^{13}C$, *Paleoceanography*, *21*, PA2012, doi:10.1029/2005PA001226.

Ruttenberg, K. C. (1993), Reassessment of the oceanic residence time of phosphorus, *Chem. Geol.*, *107*, 405–409, doi:10.1016/0009-2541(93)90220-D.

Ruttenberg, K. C. (2003), The global phosphorus cycle, in *Treatise on Geochemistry*, vol. 8, edited by W. H. Schlesinger, pp. 585–643, Elsevier, New York.

Sarnthein, M., K. Winn, J. C. Duplessy, and M. R. Fontugne (1988), Global variations of surface ocean productivity in low and mid latitudes: Influence on CO_2 reservoirs of the deep ocean and atmosphere during the last 21,000 years, *Paleoceanography*, *3*, 361–399, doi:10.1029/PA003i003p00361.

Seidov, D., M. Sarnthein, K. Stattegger, R. Prien, and M. Weinelt (1996), North Atlantic Ocean circulation during the Last Glacial Maximum and subsequent meltwater event: A numerical model, *J. Geophys. Res.*, *101*(C7), 16,305–16,332.

Siddall, M., E. J. Rohling, A. Almogi-Labin, C. Hemleben, D. Meischner, I. Schmelzer, and D. A. Smeed (2003), Sea-level fluctuations during the last glacial cycle, *Nature*, *423*, 853–858, doi:10.1038/nature01690.

Siegenthaler, U., et al. (2005), Stable carbon cycle-climate relationship during the late Pleistocene, *Science*, *310*, 1313–1317.

Sigman, D. M., and E. A. Boyle (2000), Glacial/interglacial variations in atmospheric carbon dioxide, *Nature*, *407*, 859–869, doi:10.1038/35038000.

Sigman, D. M., M. A. Altabet, D. C. McCorke, R. François, and G. Fischer (1999), The $\delta^{15}N$ of nitrate in the Southern Ocean: Consumption of nitrate in surface waters, *Global Biogeochem. Cycles*, *13*(4), 1149–1166, doi:10.1029/1999GB900038.

Sigman, D. M., S. L. Jaccard, and G. H. Haug (2004), Polar ocean stratification in a cold climate, *Nature*, *428*, 59–63, doi:10.1038/nature02357.

Slomp, C. P., and P. Van Cappellen (2007), The global marine phosphorus cycle: Sensitivity to oceanic circulation, *Biogeosciences*, *4*, 155–171.

Slomp, C. P., E. H. G. Epping, W. Helder, and W. Van Raaphorst (1996), A key role for iron-bound phosphorus in authigenic apatite formation in North Atlantic continental platform sediments, *J. Mar. Res.*, *54*, 1179–1205, doi:10.1357/0022240963213745.

Tamburini, F. (2001), Phosphorus in marine sediments during the past 150000 years: Exploring relationships between continental weathering, productivity, and climate, Ph.D. thesis, 217 pp., Univ. de Neuchatel, Neuchatel, France.

Toggweiler, J. R. (1999), Variations of atmospheric CO_2 by ventilation of the world's deepest water, *Paleoceanography*, *14*, 571–588, doi:10.1029/1999PA900033.

Tyrrell, T. (1999), The relative influence of Nitrogen and Phosphorus on oceanic primary production, *Nature*, *400*, 525–531, doi:10.1038/22941.

Van Cappellen, P., and E. D. Ingall (1994), Benthic phosphorus regeneration, net primary production and ocean anoxia: A model of the coupled marine biogeochemical cycles of carbon and phosphorus, *Paleoceanography*, *9*, 677–692, doi:10.1029/94PA01455.

Wallmann, K. (2003), Feedbacks between oceanic redox states and marine productivity: A model perspective focused on benthic phosphorus cycling, *Global Biogeochem. Cycles*, *17*(3), 1084, doi:10.1029/2002GB001968.

West, S., J. H. F. Jansen, and J.-B. Stuut (2004), Surface water conditions in the Northern Banguela region (SE Atlantic) during the last 450 ky reconstructed from assemblages of planktonic foraminifera, *Mar. Micropaleontol.*, *51*, 321–344, doi:10.1016/j.marmicro.2004.01.004.

Willamowski, C., and R. Zahn (2000), Upper ocean circulation in the glacial North Atlantic from benthic foraminiferal isotope and trace element fingerprinting, *Paleoceanography*, *15*, 515–527, doi:10.1029/1999PA000467.

Winguth, A., D. Archer, E. Maier-Reimer, and U. Mikolajewicz (2000), Paleonutrient data analysis of the glacial Atlantic using an adjoint ocean general circulation model, in *Inverse Methods in Global Biogeochemical Cycles*, *Geophys. Monogr. Ser.*, vol. 114, edited by P. S. Kasibhatla et al., pp. 171–183, AGU, Washington, D. C.

Wunsch, C. (2003), Determining paleoceanographic circulations, with emphasis on the Last Glacial Maximum, *Quat. Sci. Rev.*, *22*, 371–385, doi:10.1016/S0277-3791(02)00177-4.

Yu, E. R., R. François, and M. Bacon (1996), Similar rates of modern and last-glacial ocean thermohaline circulation inferred from radiochemical data, *Nature*, *379*, 689–694, doi:10.1038/379689a0.

C. P. Slomp, I. Tsandev, and P. Van Cappellen, Department of Earth Sciences-Geochemistry, Faculty of Geosciences, Utrecht University, P.O. Box 80.021, NL-3508 TA Utrecht, Netherlands. (i.tsandev@geo.uu.nl)